Annales Geophysicae (2002) 20: 1967–1976

Annales Geophysicae

Modelling the effects of the October 1989 solar proton event on mesospheric odd nitrogen using a detailed ion and neutral chemistry model

P. T. Verronen[1], E. Turunen[2], Th. Ulich[2], and E. Kyrölä[1]

[1]Finnish Meteorological Institute, Geophysical Research Division, P.O. Box 503, 00101 Helsinki, Finland
[2]Sodankylä Geophysical Observatory, Tähteläntie 112, 99600 Sodankylä, Finland

Received: 10 October 2001 – Revised: 22 April 2002 – Accepted: 2 July 2002

Abstract. Solar proton events and electron precipitation affect the concentrations of middle atmospheric constituents. Ionization caused by precipitating particles enhances the production of important minor neutral constituents, such as nitric oxide, through reaction chains in which ionic reactions play an important role. The Sodankylä Ion Chemistry model (SIC) has been modified and extended into a detailed ion and neutral chemistry model of the mesosphere. Our steady-state model (containing 55 ion species, 8 neutral species, and several hundred chemical reactions) is used to investigate the effect of the October 1989 solar proton event on odd nitrogen at altitudes between 50–90 km. The modelling results show that the NO concentration is significantly enhanced due to the proton precipitation, reaching 10^7–10^8 cm^{-3} throughout the mesosphere on the 20 October when the proton forcing was most severe. A comparison between the chemical production channels of odd nitrogen indicates that ion chemical reactions are an important factor in the total odd nitrogen production during intense ionization. The modelled electron concentration for the 23 October is compared with EISCAT incoherent scatter radar measurements and a reasonable agreement is found.

Key words. Atmospheric composition and structure (Middle atmosphere – composition and chemistry); Ionosphere (Particle precipitation)

1 Introduction

Energetic proton precipitation as a result of solar events can significantly increase the production of odd nitrogen through impact ionization and ion chemistry (Crutzen et al., 1975; Rusch et al., 1981). During polar night conditions, when sunlight is absent, the photolysis reactions cannot destroy odd nitrogen. Because there is no other significant loss process, odd nitrogen is long lived and can be transported into lower mesospheric and even stratospheric altitudes as well as into lower latitudes (Siskind et al., 1997; Callis and Lambeth, 1998). If transported to the stratosphere, the extra odd nitrogen could be important to the ozone balance because it reacts with ozone in one of the catalytic reaction chains that, in addition to the pure oxygen chemistry, are important to the ozone budget.

Effects of anomalously large solar proton events, such as the August 1972 and October 1989 events, on middle atmosphere have been modelled in the past (Rusch et al., 1981; Jackman and Meade, 1988; Reid et al., 1991; Jackman et al., 1995). Reid et al. (1991) estimated a factor of 20 increase in NO at 60 km and a corresponding 20% loss of ozone at 40 km in the polar cap region as a result of the October 1989 solar proton event. Similar results have been published by Jackman et al. (1995). Zadorozhny et al. (1992) have measured more than one order of magnitude increase in NO concentration at 50 km during the October 1989 solar proton event. In the modelling efforts mentioned above, ion chemistry has been included in the form of a single constant parameter that connects precipitation-induced ionization rate and atomic nitrogen production. In this approach the production rate of odd nitrogen is obtained by multiplying the ionization rate by a constant, usually between 1.2 and 1.6, which is based on theoretical studies (Porter et al., 1976; Rusch et al., 1981).

In this paper we use a detailed ion and neutral chemistry model, with 55 ion species and several hundred chemical reactions, to calculate the forcing on the mesosphere due to the October 1989 solar proton event. Our aim is to study in detail the production of odd nitrogen during the event. Using a coupled ion and neutral chemistry model means that it is not necessary for us to parameterise the chemical reaction chain between ionization and odd nitrogen production. Instead, it is possible to connect the measured proton flux and odd nitrogen production by a direct calculation. Therefore, our main new input to the study of the October 1989 SPE will be the utilisation of an extensive and detailed ion chemistry scheme.

Correspondence to: P. T. Verronen (pekka.verronen@fmi.fi)

Table 1. A list of the neutral reactions that have been added to the SIC model. The sources for the reactions and rates are DeMore et al. (1994, 1992); Brasseur and Solomon (1986), and Rees (1989). Units are $cm^3\ s^{-1}$ and $cm^6\ s^{-1}$ for second and third order reactions, respectively. T is temperature and M is any atmospheric molecule

Reaction			Reaction rate	Source
$O + O_2 + M$	$\longrightarrow$	$O_3 + M$	$6.0 \times 10^{-34} \times (300/T)^{2.3}$	DeMore 94
$O + O + M$	$\longrightarrow$	$O_2 + M$	$4.7 \times 10^{-33} \times (300/T)^{2}$	B & S 86
$O + O_3$	$\longrightarrow$	$O_2 + O_2$	$8.0 \times 10^{-12} \times e^{-2060/T}$	DeMore 94
$O + OH$	$\longrightarrow$	$O_2 + H$	$2.2 \times 10^{-11} \times e^{120/T}$	DeMore 94
$O + NO_2$	$\longrightarrow$	$NO + O_2$	$6.5 \times 10^{-12} \times e^{120/T}$	DeMore 94
$O + NO_3$	$\longrightarrow$	$NO_2 + O_2$	1.0×10^{-11}	DeMore 94
$O + HO_2$	$\longrightarrow$	$OH + O_2$	$3.0 \times 10^{-11} \times e^{200/T}$	DeMore 94
$NO + O + M$	$\longrightarrow$	$NO_2 + M$	$9.0 \times 10^{-32} \times (300/T)^{1.5}$	DeMore 92
$NO + O_3$	$\longrightarrow$	$NO_2 + O_2$	$2.0 \times 10^{-12} \times e^{-1400/T}$	DeMore 94
$NO + OH + M$	$\longrightarrow$	$HNO_2 + M$	$7.0 \times 10^{-31} \times (300/T)^{2.6}$	DeMore 92
$NO + HO_2$	$\longrightarrow$	$NO_2 + OH$	$3.7 \times 10^{-12} \times e^{250/T}$	DeMore 94
$NO + NO_3$	$\longrightarrow$	$NO_2 + NO_2$	$1.5 \times 10^{-11} \times e^{170/T}$	DeMore 94
$N + O_2$	$\longrightarrow$	$NO + O$	$1.5 \times 10^{-11} \times e^{-3600/T}$	DeMore 94
$N + NO$	$\longrightarrow$	$N_2 + O$	$2.1 \times 10^{-11} \times e^{100/T}$	DeMore 94
$N + NO_2$	$\longrightarrow$	$N_2O + O$	3.0×10^{-12}	B & S 86
$H + O_2 + M$	$\longrightarrow$	$HO_2 + M$	$5.7 \times 10^{-32} \times (300/T)^{1.6}$	DeMore 92
$H + O_3$	$\longrightarrow$	$OH + O_2$	$1.4 \times 10^{-10} \times e^{-470/T}$	DeMore 94
$H + HO_2$	$\longrightarrow$	$OH + OH$	$0.9 \times (8.1 \times 10^{-11})$	DeMore 94
$H + HO_2$	$\longrightarrow$	$H_2 + O_2$	$0.08 \times (8.1 \times 10^{-11})$	DeMore 94
$H + HO_2$	$\longrightarrow$	$H_2O + O$	$0.02 \times (8.1 \times 10^{-11})$	DeMore 94
$OH + O_3$	$\longrightarrow$	$HO_2 + O_2$	$1.6 \times 10^{-12} \times e^{-940/T}$	DeMore 94
$OH + OH$	$\longrightarrow$	$O + H_2O$	$4.2 \times 10^{-12} \times e^{-240/T}$	DeMore 94
$OH + OH + M$	$\longrightarrow$	$H_2O_2 + M$	$6.9 \times 10^{-31} \times (300/T)^{0.8}$	DeMore 92
$OH + HO_2$	$\longrightarrow$	$H_2O + O_2$	$4.8 \times 10^{-11} \times e^{250/T}$	DeMore 94
$OH + H_2$	$\longrightarrow$	$H_2O + H$	$5.5 \times 10^{-12} \times e^{-2000/T}$	DeMore 94
$OH + NO_2 + M$	$\longrightarrow$	$HNO_3 + M$	$2.6 \times 10^{-30} \times (300/T)^{3.2}$	DeMore 92
$OH + NO_3$	$\longrightarrow$	$NO_2 + HO_2$	2.2×10^{-11}	DeMore 94
$OH + HNO_2$	$\longrightarrow$	$NO_2 + H_2O$	$1.8 \times 10^{-11} \times e^{-390/T}$	DeMore 92
$OH + HNO_3$	$\longrightarrow$	$NO_3 + H_2O$	$7.2 \times 10^{-15} \times e^{785/T}$	B & S 86
$OH + H_2O_2$	$\longrightarrow$	$H_2O + HO_2$	$2.9 \times 10^{-12} \times e^{-160/T}$	DeMore 94
$NO_2 + O_3$	$\longrightarrow$	$NO_3 + O_2$	$1.2 \times 10^{-13} \times e^{-2450/T}$	DeMore 94
$HO_2 + O_3$	$\longrightarrow$	$OH + 2O_2$	$1.1 \times 10^{-14} \times e^{-500/T}$	DeMore 94
$Cl + O_3$	$\longrightarrow$	$ClO + O_2$	$2.9 \times 10^{-11} \times e^{-260/T}$	DeMore 94
$ClO + O$	$\longrightarrow$	$Cl + O_2$	$3.0 \times 10^{-11} \times e^{70/T}$	DeMore 94
$ClO + NO$	$\longrightarrow$	$NO_2 + Cl$	$6.4 \times 10^{-12} \times e^{290/T}$	DeMore 94
$O(^1D) + N_2$	$\longrightarrow$	$O + N_2$	$1.8 \times 10^{-11} \times e^{110/T}$	DeMore 94
$O(^1D) + N_2$	$\longrightarrow$	N_2O	$3.5 \times 10^{-37} \times (300/T)^{0.6}$	DeMore 94
$O(^1D) + O_2$	$\longrightarrow$	$O + O_2$	$3.2 \times 10^{-11} \times e^{70/T}$	DeMore 94
$O(^1D) + H_2O$	$\longrightarrow$	$OH + OH$	2.2×10^{-10}	DeMore 94
$O(^1D) + O_3$	$\longrightarrow$	$O_2 + O_2$	1.2×10^{-10}	DeMore 94
$O(^1D) + O_3$	$\longrightarrow$	$2O + O_2$	1.2×10^{-10}	B & S 86
$O(^1D) + H_2$	$\longrightarrow$	$OH + H$	1.0×10^{-10}	DeMore 94
$O(^1D) + N_2O$	$\longrightarrow$	$N_2 + O_2$	4.9×10^{-11}	DeMore 94
$O(^1D) + N_2O$	$\longrightarrow$	$NO + NO$	6.7×10^{-11}	DeMore 94
$N(^2D) + O_2$	$\longrightarrow$	$NO + O$	5.3×10^{-12}	Rees 89
$N(^2D) + O_2$	$\longrightarrow$	$NO + O(^1D)$	5.3×10^{-12}	Rees 89
$N(^2D) + O$	$\longrightarrow$	$N + O$	2.0×10^{-12}	Rees 89
$N(^2D) + NO$	$\longrightarrow$	$N_2 + O$	7.0×10^{-11}	Rees 89

Table 2. The branching ratios for the reactions producing $N(^2D)$

Reaction			Ratio	Source
$p^* + N_2$ (impact)	$\longrightarrow$	$N + N^+ + e$	0.50	Porter et al. (1976)
$N_2 + h\nu$	$\longrightarrow$	$N + N$	0.50	Marov et al. (1996)
$N^+ + O_2$	$\longrightarrow$	$N + O_2^+$	0.65	Rees (1989)
$N_2^+ + O$	$\longrightarrow$	$N + NO^+$	1.00	Marov et al. (1996)
$N_2^+ + e$ (recomb.)	$\longrightarrow$	$N + N$	0.50	Marov et al. (1996)
$NO^+ + e$ (recomb.)	$\longrightarrow$	$N + O$	0.78	Marov et al. (1996)

2 The Sodankylä Ion Chemistry model

The Sodankylä Ion Chemistry (SIC) model was developed as an alternative approach to the D-region ion chemistry models that connect chemical reactions to effective parameters which are set against experimental data. A detailed chemical scheme, in a conceptually simple model, was built to be a tool for interpretation of D-region incoherent scatter experiments and cosmic radio noise absorption measurements. The SIC model was first applied by Burns et al. (1991) in a study of incoherent scatter radar measurements. Since then, the SIC model has been used in many scientific studies (Turunen, 1993; Rietveld et al., 1996; Ulich et al., 2000). A detailed description of the model is given by Turunen et al. (1996).

Originally the model was developed for geophysically quiet conditions. Consequently, the solar radiation (5–135 nm) and galactic cosmic radiation (GCR) were considered as ionization sources acting on five primary neutral components. Later, the model was extended to include electron and proton precipitation as ionization sources.

The SIC model can be run either in a steady-state or time-dependent mode. The model solves for the concentrations of 55 ions (36 positive, 19 negative) in the ionospheric D-region. Local chemical equilibrium can be calculated in the altitude range from 50 to 100 km with 1 km resolution. The solution for the steady state can be advanced in time, so that the response of the ion concentrations to sudden changes, such as sunrise/sunset conditions or particle events, can be studied in detail. Mathematically SIC is zero dimensional because transport processes are not included in the model.

The SIC model is based on the latest knowledge of detailed ion composition and the mutual reactions of the ions in the lower ionosphere; it uses background neutral atmospheres provided by the MSISE-90 model (Hedin, 1991), and fixed information about solar irradiance (Heroux and Hinteregger, 1978; Torr et al., 1979). Additionally, SIC can use fixed minor neutral constituent profiles, including O, $O(^1D)$, $O_2(1\Delta_g)$, O_3, N, NO, NO_2, NO_3, N_2O, N_2O_2, H_2, H, OH, H_2O, HO_2, HNO_2, HNO_3, HCl, Cl, ClO, CH_3, CH_4, CO_2, and CO_3, as given by e.g. Shimazaki (1984). The ionization rate due to the galactic cosmic radiation is calculated using a parameterisation by Heaps (1978), and the ionization rate due to proton precipitation according to Reid (1961). The ionization rates due to solar UV and electron precipitation are calculated following Rees (1989).

Table 3. The dissociation processes included in the SIC model

O_2	+	$h\nu$	$\longrightarrow$	O	+	$O/O(^1D)$
O_3	+	$h\nu$	$\longrightarrow$	$O/O(^1D)$	+	$O_2/O_2(^1\Delta_g)$
N_2	+	$h\nu$	$\longrightarrow$	N	+	N
NO	+	$h\nu$	$\longrightarrow$	N	+	O
NO_2	+	$h\nu$	$\longrightarrow$	NO	+	O
H_2O	+	$h\nu$	$\longrightarrow$	OH	+	H

2.1 The neutral chemistry included in the SIC model

In order to investigate the effects of particle precipitation on the middle atmospheric odd nitrogen, the ion chemistry has to be coupled with relevant neutral chemistry. With the intention of including all the components and reactions needed to chemically connect the ions with the odd nitrogen species, we have added 48 reactions of O, $O(^1D)$, O_3, H, OH, N, $N(^2D)$, and NO to the chemical scheme. These reactions, see Table 1, are well known and documented in standard literature. The $N(^2D)$ branching ratios used are listed in Table 2. In the original model, concentrations of neutral species were fixed, so the model code has been modified to treat the eight neutrals mentioned above as unknowns.

In addition to photoionization, the photodissociation processes of N_2, O_2, O_3, H_2O, NO, and NO_2 have been included in the model (see Table 3). In order to do this, the wavelength range of solar radiation was extended from the original ionization region of 5–135 nm and now includes also the region between 135–422 nm. The sources of absorption cross sections and solar flux data are listed in Table 4. Because of a complex overlap of the O_2 and NO absorption bands, the NO dissociation rate is calculated using opacity distribution functions (Minschwaner and Siskind, 1993). The N_2 dissociation rate is calculated according to Rees (1989). The quantum yield of O_3 dissociation between O + O_2 and $O(^1D)$ + $O_2(^1\Delta_g)$ around 310 nm as well as the NO_2 quantum yield are considered according to DeMore et al. (1992).

2.2 Calculating the forcing due to precipitating protons

There are several methods that can be used to calculate the energy input of protons and the resulting ionization rate in the atmosphere. Decker et al. (1996) have presented a comparison of three different modelling approaches: Monte Carlo, linear transport, and continuously slowing-down approximation. They found an excellent agreement between the three methods except for the cases where protons had penetrated

Table 4. The sources for the absorption cross sections/dissociation efficiencies and solar flux data

	Wavelength	Source
Solar flux	135.0–175.0 nm	(Shimazaki, 1984)
	175.0– 422.5 nm	(WMO, 1985)
O_2 abs.	135.0–175.0 nm	(Shimazaki, 1984)
	175.0–422.5 nm	(WMO, 1985)
O_3 abs.	135.0–175.0 nm	(Shimazaki, 1984)
	175.4–422.5 nm	(WMO, 1985)
N_2 abs.	65.0–102.6 nm	(Rees, 1989)
NO abs.	181.6–192.5 nm	(Minschwaner and Siskind, 1993)
NO_2 abs.	135.0–175.0 nm	(Shimazaki, 1984)
	202.0–422.5 nm	(DeMore et al., 1992)
H_2O abs.	175.5–189.3 nm	(DeMore et al., 1992)

Table 5. Photochemical time constants at noon (Shimazaki, 1984)

Constituent	50 km	80 km	100 km
O	10 s	3.5 h	116 d
O_3	2 min	1 min	1 min
N	4.6 s	5 h	4.5 d
NO	14 min	18 h	2 d
NO_2	10 s	3 s	1.5 s
H	0.1 s	44 min	12 d
OH	3.2 s	0.7 s	0.3 s

Table 6. Characteristic transport lifetimes (Brasseur and Solomon, 1986)

Transport type	50 km	80 km	100 km
Zonal ($\bar{u}$)	5 h	18 h	42 h
Meridional ($\bar{v}$)	370 h	76 h	220 h
Vertical ($\bar{w}$)	890 h	890 h	570 h
Diffusion	370 h	76 h	34 h

so deep that their fluxes were significantly modified, which happens well below the bulk ionization region. However, the effects of magnetic mirroring and lateral spreading of H^+/H flux were turned off in the Monte Carlo calculations because the other two methods do not take these effects into account.

Our current calculation is based on the energy-range measurements in standard air for protons by Bethe and Ashkin (1953). We also require a proton spectrum and a neutral atmosphere in order to calculate the ionization rate. First we calculate the deposition rate of energy at each altitude, using a calculation algorithm originally presented by Reid (1961).

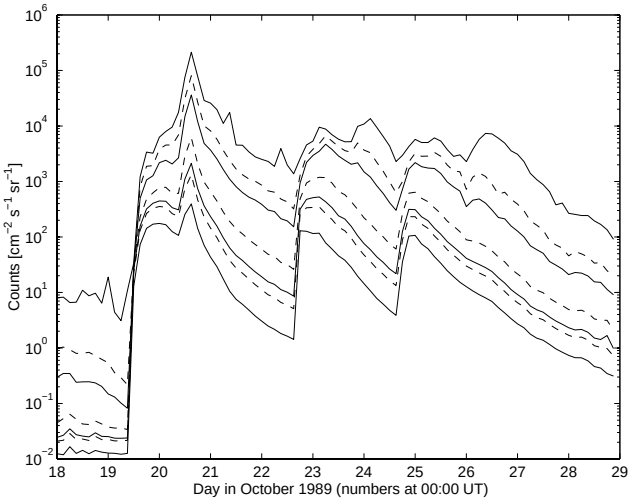

Fig. 1. Integrated proton fluxes for late October 1989 (obtained from the World Wide Web server for the NOAA National Geophysical Data Center), showing three-hour averages of the seven energy channels of the GOES satellite proton measurements. From top curve down the channels are: >1, >5, >10, >30, >50, >60, and >100 MeV.

Next we divide the deposited energy by the average energy loss per ion pair formation, taken to be 36 eV (see e.g. Rees, 1989, p. 40), to get the total ionization rate. The total ionization rate is then divided between the three major constituents (i.e. N_2, O_2, and O) according to their relative concentrations and cross sections (Rees, 1982). Finally, we further divide the ionization rates of individual constituents between the ionization and dissociative ionization processes using the branching ratios given by Jones (1974) to obtain the production/loss rates for the individual ions and neutrals.

Protons can undergo charge-exchange reactions with the neutral molecules. However, to reach the atmospheric altitude region between 100 and 50 km a proton must possess an initial energy between $\sim$100 keV and $\sim$30 MeV. At these energies the charge-exchange reactions are not important. Further, because of the high energy of these protons their stopping power is due to ionising collisions only (Rees, 1982). Therefore, we have ignored the direct dissociation by protons. Our calculations do not include dissociation by secondary electrons. Recently, Solomon (2001) has studied ionization by secondary electrons during proton aurora at altitudes above 80 km. He showed that the secondary electrons become progressively more important as the primary proton energy increases. The secondary electrons are an important factor in odd nitrogen production because they dissociate N_2. We will estimate the error due to exclusion of secondary electrons in Sect. 5.

3 Modelling the October 1989 solar proton event

In 1989, at the peak of solar maximum, there were several large solar proton events (SPE), e.g. in August, October, and

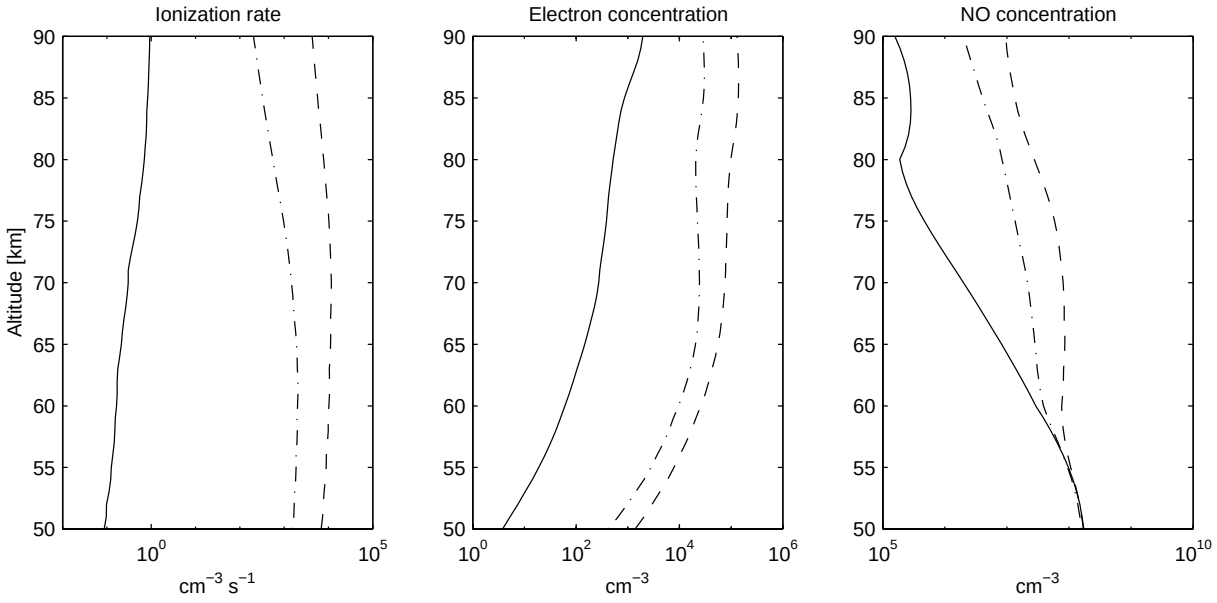

Fig. 2. The modelled ionization rate, electron concentration, and NO concentration profiles during the October 1989 SPE. Solid lines are for the 18, dashed lines for the 20 and dash-dot lines for the 23 October.

November. In this work we model the proton event that started on 19 October 1989, had peaks on the 20, 23, and 25 October, and then decayed away. This particular SPE is one of the biggest proton events to date and it provided an extreme forcing on the middle atmosphere. Therefore, it is a good choice for a maximum effect study. The EISCAT incoherent scatter radar was operated during the event, so that we are able to compare ground-based measurements of electron concentration with our modelling results. This was another reason for choosing this particular event.

The proton flux data from the GOES-7 satellite measurements for the October 1989 SPE, see Fig. 1, were obtained from the World Wide Web server for the NOAA National Geophysical Data Center at www.ndgc.noaa.gov/stp/stp.html. The GOES measurements were converted to differential proton flux for 600 keV–2000 MeV range assuming that the flux can be described by the exponential rigidity relation (Freier and Webber, 1963). Because of the high magnetic latitude of our calculation point (66.46° N), virtually all protons are able to enter the atmosphere (see e.g. Hargreaves, 1992, p. 358). Therefore, the proton spectra at the top of the atmosphere are assumed to be the same as those measured by GOES at the geosynchronous altitude. In near-Earth space protons are found to be travelling in all directions (see e.g. Hargreaves, 1992, p. 354). For this reason, we have assumed that the angular distribution of protons is isotropic over the upper hemisphere, i.e. when calculating the ionization by protons at each altitude point, we assume that the protons can enter, if possessing enough energy, from any direction with pitch angle less than 90°. Neither magnetic mirroring effects nor further pitch angle limits were considered.

For each day between the 18 and 28 October, we calculated the MSISE-90 temperature and neutral concentration profiles at 12:00 UT over Tromsø (69.59° N, 19.23° E). The minor profiles that are not provided by the MSISE-90 model were taken from Shimazaki (1984). We then calculated the corresponding production and loss rates of individual ions and neutrals due to photoionization and photodissociation. We also calculated an average proton flux between 12:00 and 15:00 UT and the corresponding ion production rates due to proton penetration. Using these production rates we then calculated the steady-state concentrations for ions and selected neutrals taking into account the production and loss in ion/neutral chemical reactions.

During daytime, i.e. when solar radiation is present, and at mesospheric altitudes it is reasonable to assume a steady-state condition for the ions and most of the modelled neutral constituents because their chemical time constants (see Table 5) are shorter than the solar-illuminated period of the day, which is roughly 8–10 h for our calculation points. NO is the one exception with a chemical time constant of 18 h at 80 km. Therefore, our results for NO actually compare the production environment from day to day showing the local forcing on NO, i.e. a state that would eventually be reached if the conditions would remain the same.

We are ignoring transport effects in this study. The characteristic transport lifetimes are generally much greater than the photochemical time constants (Table 6). In zonal direction this is not the case at 50 km altitude. However, in the case of solar proton events (also known as polar cap absorption or PCA events), unlike the case of highly localised high energy electron precipitation, the effects cover the whole polar cap area above a certain magnetic latitude (Hargreaves, 1992). Hence, we assume that we have similar particle forcing conditions in the zonal regions surrounding our calculation spot. Further, the general meridional wind direction on

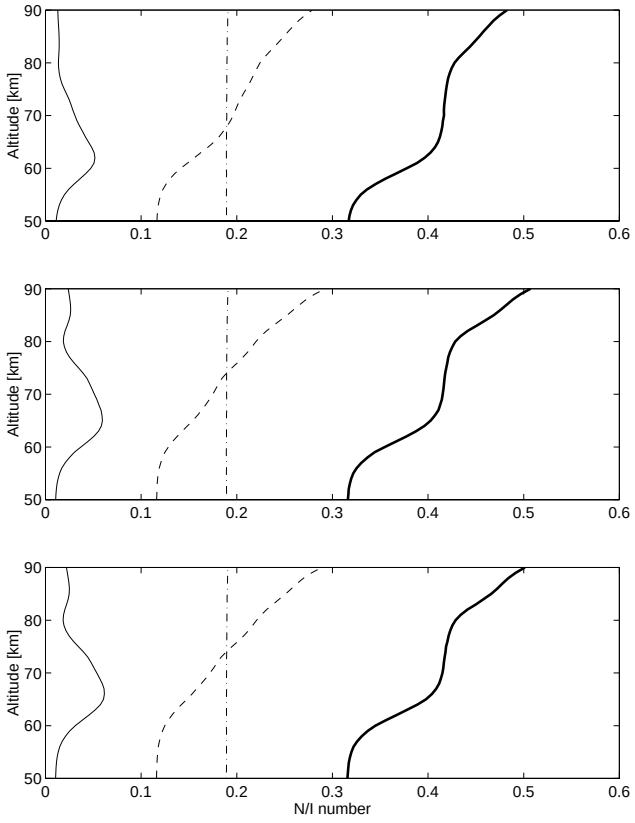

Fig. 3. The N/I number, i.e. the number of odd nitrogen species ($N(^4S)$, $N(^2D)$ and NO) created per ion pair produced by proton impact. From the top downwards the panels are for the 20, 23, and 25 October 1989. The total number is shown with the bold solid line. The dash-dot, dashed and solid lines show the contributions by dissociative ionization, ionic production of atomic nitrogen and ionic production of NO, respectively. The contribution of secondary electrons is not taken into account.

our calculations spot (69.59° N, winter hemisphere) is from north to south, thus the wind is bringing in material from the affected polar cap area. Therefore, we assume that horizontal transport does not significantly affect our results in time scales of hours.

It should be noted that our calculations extend up to 90 km. We are showing all the results to get a larger picture, but one should remember that the steady-state approach gets progressively more questionable above 80 km when calculating NO concentrations.

4 Results

Figure 2 shows the variations of the ionization rate, electron concentration and NO concentration during the SPE. The electron and NO variations follow the ionization rate variations. On the 20 October, when the proton flux peaks, we find that the ionization rate can be 7.9×10^4 times, the electron concentration 430 times, and the NO concentration 160 times as large as the background values on the 18 October.

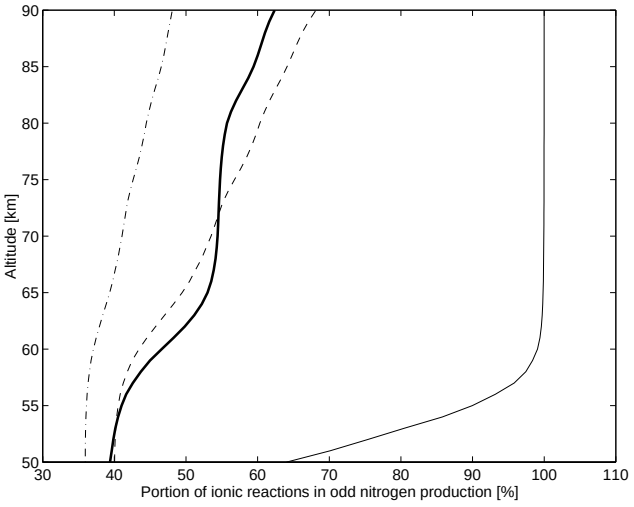

Fig. 4. The portion of ions in $N(^4S)$, $N(^2D)$, NO and total odd nitrogen production represented by dash-dot, dashed, solid and bold solid lines, respectively. These curves are for the 23 October 1989. The contribution of secondary electrons is not taken into account.

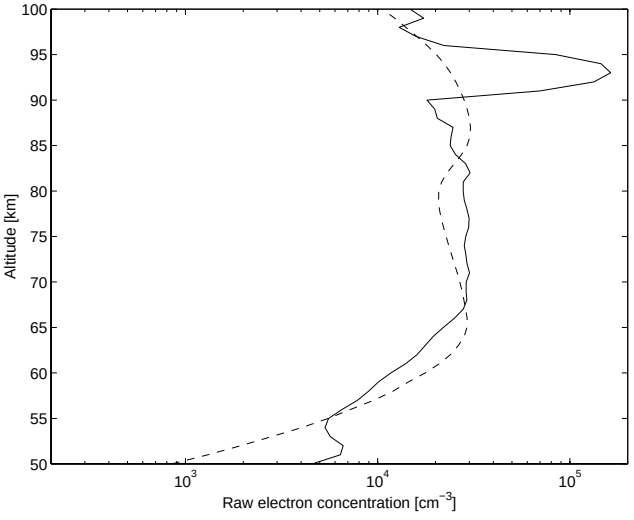

Fig. 5. The electron concentration profiles for the 23 October 1989 as modelled by SIC (the dashed line) and measured by EISCAT (the solid line). The modelled curve is for 12:00 UT, while EISCAT curve is an average of the measurements made between 12:00 and 14:00 UT.

The same values for the 23 October are 1.8×10^4, 160, and 45, respectively. For both cases the increase of ionization peaks at 50 km and the increase of electron concentration at 60 km. The increase of NO concentration peaks at 78 and 79 km on 20 and 23 October, respectively. The extreme enhancements on the 20 October are caused by a sharp peak of the proton flux, located between 12:00 and 15:00 UT (Fig. 1).

For NO, smaller changes were predicted by Reid et al. (1991), who used a 2-D time-dependent model to study the 1989 SPE and obtained the largest NO increases, up to a factor of 20, in the end of October between 60 and 80 km.

Table 7. The ionic reactions producing odd nitrogen. The sources of the reaction rates are listed by Turunen et al. (1996), except for † and †† which are taken from Matsuoka et al. (1981) and Rees (1989), respectively

Reaction			Rate	
$O^+ + N_2$	$\longrightarrow$	$N + NO^+$	$1.2 \times 10^{-12} \times (300/T)$	
$O_2^+ + N_2$	$\longrightarrow$	$NO + NO^+$	2×10^{-18}	†
$N^+ + O_2$	$\longrightarrow$	$N + O_2^+$	1.1×10^{-10}	
$N^+ + O_2$	$\longrightarrow$	$N(^2D) + O_2^+$	2.0×10^{-10}	
$N^+ + O_2$	$\longrightarrow$	$NO + O^+$	3.0×10^{-11}	
$N^+ + O$	$\longrightarrow$	$N + O^+$	5.0×10^{-13}	
$N^+ + e$	$\longrightarrow$	N	1.0×10^{-12}	
$N_2^+ + O$	$\longrightarrow$	$N(^2D) + NO^+$	$1.4 \times 10^{-10} \times (300/T)^{4.4}$	
$N_2^+ + e$	$\longrightarrow$	$N + N(^2D)$	$1.8 \times 10^{-7} \times (300/T)^{0.39}$	††
$NO^+ + e$	$\longrightarrow$	$N + O$	$0.22 \times 4.2 \times 10^{-7} \times (300/T)^{0.85}$	
$NO^+ + e$	$\longrightarrow$	$N(^2D) + O$	$0.78 \times 4.2 \times 10^{-7} \times (300/T)^{0.85}$	
$NO^+(N_2) + e$	$\longrightarrow$	$NO + N_2$	$1.4 \times 10^{-6} \times (300/T)^{0.4}$	
$NO^+(CO_2) + e$	$\longrightarrow$	$NO + CO_2$	1.5×10^{-6}	
$NO^+(H_2O) + e$	$\longrightarrow$	$NO + H_2O$	1.5×10^{-6}	
$NO^+(H_2O) + H$	$\longrightarrow$	$NO + H^+(H_2O)$	7×10^{-12}	
$NO^+(H_2O)_2 + e$	$\longrightarrow$	$NO + 2H_2O$	2.0×10^{-6}	
$NO^+(H_2O)_3 + e$	$\longrightarrow$	$NO + 3H_2O$	2.0×10^{-6}	
$NO^+(H_2O)(N_2) + e$	$\longrightarrow$	$NO + H_2O + N_2$	3.0×10^{-6}	
$NO^+(H_2O)(CO_2) + e$	$\longrightarrow$	$NO + H_2O + CO_2$	3.0×10^{-6}	
$NO^+(H_2O)_2(N_2) + e$	$\longrightarrow$	$NO + 2H_2O + N_2$	3.0×10^{-6}	
$NO^+(H_2O)_2(CO_2) + e$	$\longrightarrow$	$NO + 2H_2O + CO_2$	3.0×10^{-6}	

Zadorozhny et al. (1992) made a rocket measurement on the 23 October 05:00 UT in the southern part of Indian Ocean (geomagnetic latitude 60° S) and reported more than one order of magnitude increase in the NO concentration, compared to measurements on the 11 and 12 October. They found the largest increases at 50 km altitude. In our calculations, the absolute NO values for the 23 October vary between 1.5×10^8 and 1.5×10^6 while Zadorozhny et al. (1992) report values between $\sim 2 \times 10^9$ and $\sim 2 \times 10^8$. Therefore, the larger change in our calculations is not due to larger values during the event but rather because of smaller reference values. The main reason for the smaller reference values is the fact that our calculations do not take into account the precipitation history before the 18 October, while the measurements by Zadorozhny et al. (1992) are affected by earlier particle events.

Figure 3 shows the N/I number, i.e. the number of odd nitrogen species ($N(^4S)$, $N(^2D)$ and NO) produced per each ion pair, on the 20, 23 and 25 October. The altitude profiles show similar behaviour, a variation between 0.31 and 0.51. Theoretical calculations (Porter et al., 1976; Rusch et al., 1981) predict that 1.2–1.6 nitrogen atoms are produced per each ion pair. However, these are not directly comparable with our results because of different production mechanisms. Porter et al. (1976) included dissociative ionization by protons and dissociation by secondary electrons, Rusch et al. (1981) included the same ones as Porter et al. (1976) and also chemical production from N^+ and O^+ while our number includes dissociative ionization by protons and production from ionic reactions but neglects N_2 dissociation by secondary electrons.

Figure 3 shows that under the forcing of energetic proton precipitation the ionic reactions produce a significant amount of odd nitrogen in the form of atomic nitrogen and NO. Table 7 lists the ionic reactions producing odd nitrogen and Fig. 4 shows the portion of the ions in the odd nitrogen production. On the 23 October, 39%–63% of the total odd nitrogen production is due to ionic reactions (note that we are neglecting the production by secondary electrons). The rest is produced by dissociative ionization of N_2 due to proton impact, N_2 photodissociation (negligible in the mesosphere) and the reaction $O(^1D) + N_2O \longrightarrow NO + NO$ (in the lower mesosphere). When calculating the ratios we have ignored the reactions between the odd nitrogen species, i.e. $N(^4S)$, $N(^2D)$, NO and NO_2.

4.1 A comparison with EISCAT measurements

Figure 5 shows a comparison between the calculated electron concentration profile and EISCAT incoherent scatter radar measurements. On the 23 October 1989 the EISCAT VHF radar was operated in a special D-region mode GEN-11, which is described in detail by Pollari et al. (1989). The altitude region normally measured is from 70 to 113 km, with 1.05 km resolution, for a vertical antenna. This time the antenna was tilted towards north so that the lowest measurable altitude was 50 km. However, measurements below 54 km

are not reliable because of the instrumental limitations (Collis and Rietveld, 1990). The EISCAT profile presented in Fig. 5 is an average of measurements done between 12:00 UT and 14:00 UT on the 23 October 1989. The solar zenith angle varied between 82.7 and 89.0°, thus the measurements were sunlit. The measured and modelled profiles clearly have the same magnitude but there are also differences between them. From 66 to 87 km we have good agreement with maximum difference less than 30%. Above 90 km there is a large peak in EISCAT electron concentration that our model does not predict. Between 56 and 67 km our model predicts larger electron concentrations than the measurements, so that at 60 km there are 51% more electrons in our model. The statistical error in EISCAT measurements is typically less than 10%.

At the upper altitude limit we would expect the measurements to show higher electron concentrations than our model calculation because we are ignoring the effect of precipitating electrons as an ionising factor. The shape of the EISCAT electron concentration profile between 90 and 95 km resembles the one measured for neutral metallic atoms at these altitudes (Plane et al., 1999). Therefore, the electron concentration peak might be a result of precipitation induced ionization in such a layer. At lower altitudes, we would expect the measurements to show less electrons than our model because in our calculations we are using all proton energy for ionization of neutral gases, thus ignoring the energy transfer to secondary electrons which gain in number as altitude decreases.

5 Discussion

Recent observational analyses have shown that as a result of particle precipitation events a significant amount of odd nitrogen is created in the mesosphere and lower thermosphere (Callis and Lambeth, 1998). According to model studies a large enough part of the created odd nitrogen is transported to lower altitudes and latitudes during winter and early spring, so that it is necessary to take into account this highly variable natural source of odd nitrogen in stratospheric ozone simulations (Callis, 2001). First and an important step in this task is to model accurately how the ambient atmosphere responds to particle forcing, requiring consideration of particle flux degrading, ionization of neutral atmosphere and ion chemistry. Many modelling efforts include the ion chemistry by using simple parameterisation that might not be sufficient to present the complex chemical scheme. In this work we have used a detailed ion chemistry scheme to study the response of odd nitrogen to the October 1989 solar proton event in the mesosphere. Also, we have made a comparison between our results and commonly used parameterisation of atomic nitrogen production.

Our model calculations show that odd nitrogen is considerably enhanced in the mesosphere as the result of a solar proton event. During the event, when intense ionization conditions prevail, ionic reactions produce a significant fraction of atomic nitrogen and a major fraction of nitric oxide. Thus, the production by ionic sources not only competes but overcomes the direct production by precipitating protons. This is the main result of this study and means that the modelling approach in which the ion chemistry is taken into account by connecting total ionization rate with neutral atomic nitrogen production neglects a significant source of odd nitrogen. Therefore, we conclude that ion chemistry, at least for the main ions, should be explicitly included if realistic modelling of particle effects is attempted.

We found that the number of odd nitrogen species produced per ion pair is not a constant but varies with altitude. This number variation makes sense because the parameters that affect the chemical scheme, such as temperature and gas concentrations, can have large altitude dependent gradients. Before making any further conclusions in this matter, we want to include the dissociation effects of secondary electrons in our model. However, based on Monte Carlo calculations for the 23 October 1989 (V. I. Shematovich and D. V. Bisikalo, private communication), we assume that the inclusion of secondary electrons affects our results only in the lower mesosphere.

A comparison between the modelled electron concentration profile and EISCAT incoherent scatter radar measurements showed a reasonable agreement. This implies that the ion photochemistry in our model is reasonably realistic. It does not directly validate the modelled neutral concentrations. In the near future we will be able to compare our modelling results with satellite measurements of mesospheric neutral constituents. This will be a better test of our model.

We estimate that in our calculations the greatest errors are due to the exclusion of secondary electrons, the ionization rate calculation method, and the uncertainty in the $N(^2D)$ branching ratios. The exclusion of transport is not as important a source of error because the transport lifetimes are relatively long and also because the prevailing wind direc-

Table 8. The maximum error estimates for the values presented in Fig. 2 (NO, for nitric oxide), Fig. 3 (N/I, for the total number), and Fig. 4 (Ionic, for the total number). The effect of uncertainty of $N(^2D)$ branching ratio was studied by changing the ratio of $NO^+ + e \longrightarrow N(^4S)/N(^2D) + O$ from 0.78 to 0.6

Error source	NO	N/I	Ionic
Ionization rate calculation method	−35%	±3%	±2%
Uncertainty of $N(^2D)$ branching ratio	−15%	+2%	+1%
Exclusion of secondary electrons at 50 km	+5%	+550%	−85%
Exclusion of secondary electrons at 60 km	+20%	+100%	−50%
Exclusion of secondary electrons at 70 km	+10%	+20%	−15%

tion at the place and time of our calculation is from the polar cap area southwards. Based on Monte Carlo calculations for the 23 October 1989 (V. I. Shematovich and D. V. Bisikalo, private communication), we can estimate the errors due the ionization rate calculation method and the exclusion of secondary electrons. Our calculation gives 40–200% higher ionization rates than the Monte Carlo method. The reason for this difference might be that a part of the energy of the primary protons is transferred to the secondary electrons, which is not considered in our calculations. The Monte Carlo results show that, at least for the case of the 23 October 1989, the secondary electrons have largest effect in the lower mesosphere and below and that their significance rapidly decreases with increasing altitude. The NO concentration can be very sensitive to the $N(^2D)$ branching ratios. For example, Barth (1992) found that a change in the ratio from 0.75 to 0.6 in recombination reaction $NO^+ + e \longrightarrow N + O$ caused a change of -100% in the nitric oxide concentration at 105 km. We did a series of sensitivity calculations and in Table 8 we summarise the resulting estimates of maximum error.

During the course of this work we developed the Sodankylä Ion Chemistry model to an ion and neutral chemistry model of the mesosphere. The SIC model does not try to compete with multidimensional models (Siskind et al., 1997; Callis et al., 1998; Jackman et al., 1995) that are used for long-term global studies. The strength of SIC is in extensive ion chemistry through which it can provide a detailed picture of short-term local perturbations. Similar extensive ion chemistry models have been used also by Kull et al. (1997) and Beig and Mitra (1997) to study lower-latitude D-region and long-term effects of greenhouse gases in the middle atmosphere, respectively. However, as far as we know, such a detailed ion chemistry scheme has not been used to address the particle precipitation problem before. The new SIC model is not perfect. We are still missing some input that would make our calculation more realistic, such as solar X-rays and secondary electrons. Our neutral chemistry is incomplete in the sense that we have only included photolysis processes and chemical reactions necessary for this work. We don't have transport in our model, a fact that restricts the realistic model calculation period.

SIC can also be used as a time-dependent model. Our near future plans include developing and using the time-dependent version of our model to study the accumulation of NO during the whole duration of a solar proton event. With the time-dependent model we will be able to study the response of the mesosphere to rapidly changing particle flux and sunrise/sunset conditions.

This work has been done as a part of the CHAMOS (CHemical Aeronomy in the Mesosphere and Ozone in the Stratosphere) study. The aim of the study is to use a large variety of satellite and ground-based measurement data together with SIC model to study the effects of energetic particle precipitation on the middle atmospheric NO and ozone. For more information about CHAMOS, see Verronen et al. (1999).

Acknowledgements. The work of P. T. V. was supported by the Academy of Finland (Finnish Graduate School in Astronomy and Space Physics). EISCAT is an International Association supported by Finland (SA), France (CNRS), the Federal Republic of Germany (MPG), Japan (NIPR), Norway (NFR), Sweden (NFR) and the United Kingdom (PPARC).

References

Barth, C. H.: Nitric oxide in the lower thermosphere, Planet. Space Sci., 40, 315–336, 1992.

Beig, G. and Mitra, A. P.: Atmospheric and ionospheric response to trace gas perturbations through ice age to the next century in the middle atmosphere. Part II - ionization, J. Atmos. Terr. Phys., 59, 1261–1275, 1997.

Bethe, A. H. and Ashkin, J.: Passage of Radiations through Matter, vol. 1 of Experimetal Nuclear Physics, (Ed) Segre, E., pp. 166–251, John Wiley & Sons, Inc., New York, USA, 1953.

Brasseur, G. and Solomon, S.: Aeronomy of the Middle Atmosphere, D. Reidel Publishing Co., Dordrecht, Holland, 1986.

Burns, C. J., Turunen, E., Matveinen, H., Ranta, H., and Hargreaves, J. K.: Chemical modeling of the quiet summer D- and E-regions using EISCAT electron density profiles, J. Atmos. Terr. Phys., 53, 115–134, 1991.

Callis, L. B.: Stratospheric studies consider crucial question of particle precipitation, EOS, 82, 297–301, 2001.

Callis, L. B. and Lambeth, J. D.: NO_y formed by precipitating electron events in 1991 and 1992: Descent into the stratosphere as observed by ISAMS, Geophys. Res. Lett., 25, 1875–1878, 1998.

Callis, L. B., Baker, D. N., Natarajan, M., Blake, J. B., Mewaldt, R. A., Selesnick, R. S., and Cummings, J. R.: A 2-D model simulations of downward transport of NO_y into the stratosphere: Effects on the 1994 austral spring O_3 and NO_y, Geophys. Res. Lett., 25, 1875–1878, 1998.

Collis, P. N. and Rietveld, M. T.: Mesospheric observations with the EISCAT UHF radar during polar cap absorption events: 1. electron densities and negative ions, Ann. Geophysicae, 8, 809–824, 1990.

Crutzen, P. J., Isaksen, I. S. A., and Reid, G. C.: Solar proton events: stratospheric sources of nitric oxide, Science, 189, 457–458, 1975.

Decker, D. T., Kozelov, B. V., Basu, B., Jasperse, J. R., and Ivanov, V. E.: Collisional degradation of the proton-H atom fluxes in the atmosphere: A comparison of theoretical techniques, J. Geophys. Res., 101, 26 947–26 960, 1996.

DeMore, W. B., Sander, S. P., Golden, D. M., Hampson, R. F., Kurylo, M. J., Howard, C. J., Ravishankara, A. R., Kolb, C. E., and Molina, M. J.: Chemical Kinetics and Photochemical Data for Use in Stratospheric Modeling, JPL Publication 92-20, Jet Propulsion Laboratory, California Institute of Technology, Pasadena, USA, 1992.

DeMore, W. B., Sander, S. P., Golden, D. M., Molina, M. J., Hampson, R. F., Kurylo, M. J., Howard, C. J., and Ravishankara, A. R.: Chemical Kinetics and Photochemical Data for Use in Stratospheric Modeling, JPL Publication 90-1, Jet Propulsion Laboratory, California Institute of Technology, Pasadena, USA, 1994.

Freier, P. S. and Webber, W. R.: Exponential rigidity spectrums for solar-flare cosmic rays, J. Geophys. Res., 68, 1605–1629, 1963.

Hargreaves, J. K.: The solar-terrestrial environment, Cambridge University Press, Cambridge, UK, 1992.

Heaps, M. G.: Parameterization of the cosmic ray ion-pair production rate above 18 km, Planet. Space Sci., 26, 513–517, 1978.

Hedin, A. E.: Extension of the MSIS thermospheric model into the middle and lower atmosphere, J. Geophys. Res., 96, 1159+, 1991.

Heroux, L. and Hinteregger, H. E.: Aeronomical reference spectrum for solar UV below 2000 å, J. Geophys. Res., 83, 5305–5308, 1978.

Jackman, C. H. and Meade, P. E.: Effect of solar proton events in 1972 and 1979 on the odd nitrogen abundance in the middle atmosphere, J. Geophys. Res., 93, 7084–7090, 1988.

Jackman, C. H., Cerniglia, M. C., Nielsen, J. E., Allen, D. J., Zawodny, J. M., McPeters, R. D., Douglas, A. R., Rosenfield, J. E., and Hood, R. B.: Two-dimensional and three-dimensional model simulations, measurements, and interpretation of the October 1989 solar proton events on the middle atmosphere, J. Geophys. Res., 100, 11 641–11 660, 1995.

Jones, A. V.: Aurora, D. Reidel Publishing Co., Dordrecht, Holland, 1974.

Kull, A., Kopp, E., Granier, C., and Brasseur, G.: Ions and electrons of the lower-latitude D-region, J. Geophys. Res., 102, 9705–9716, 1997.

Marov, M. Y., Shematovich, V. I., and Bisicalo, D. V.: Nonequilibrium aeronomic processes – a kinetic approach to the mathematical modeling, Space Science Reviews, 76, 1–204, 1996.

Matsuoka, S., Nakamura, H., and Tamura, T.: Ion-molecule reactions of N_3^+, N_4^+, O_2^+, and NO_2^+ in nitrogen containing traces of oxygen, J. Chem. Phys., 75, 681–689, 1981.

Minschwaner, K. and Siskind, D. E.: A new calculation of nitric oxide photolysis in the stratosphere, mesosphere, and lower thermosphere, J. Geophys. Res., 98, 20 401–20 412, 1993.

Plane, J. M. C., Cox, R. M., and Rollason, R. J.: Metallic layers in the mesopause and lower thermosphere region, Adv. Space Res., 24, 1559–1570, 1999.

Pollari, P., Huuskonen, A., Turunen, E., and Turunen, T.: Range ambiguity effects in a phase coded D-region incoherent scatter radar experiment, J. Atmos. Terr. Phys., 51, 937–945, 1989.

Porter, H. S., Jackman, C. H., and Green, A. E. S.: Efficiencies for production of atomic nitrogen and oxygen by relativistic proton impact in air, J. Chem. Phys., 65, 154–167, 1976.

Rees, M. H.: On the interaction of auroral protons with the Earth's atmosphere, Planet. Space Sci., 30, 463–472, 1982.

Rees, M. H.: Physics and chemistry of the upper atmosphere, Cambridge University Press, Cambridge, UK, 1989.

Reid, G. C.: A study of the enhanced ionization produced by solar protons during a polar cap absorbtion event, J. Geophys. Res., 66, 4071–4085, 1961.

Reid, G. C., Solomon, S., and Garcia, R. R.: Response of the middle atmosphere to the solar proton events of August–December, 1989, Geophys. Res. Lett., 18, 1019–1022, 1991.

Rietveld, M. T., Turunen, E., Matveinen, H., Goncharov, N. P., and Pollari, P.: Artificial periodic irregularities in the auroral ionosphere, Ann. Geophysicae, 14, 1437–1453, 1996.

Rusch, D. W., Gérard, J.-C., Solomon, S., Crutzen, P. J., and Reid, G. C.: The effect of particle precipitation events on the neutral and ion chemistry of the middle atmosphere, Planet. Space Sci., 29, 767–774, 1981.

Shimazaki, T.: Minor Constituents in the Middle Atmosphere (Developments in Earth and Planetary Physics, No 6), D. Reidel Publishing Co., Dordrecht, Holland, 1984.

Siskind, D. E., Bacmeister, J. T., Summers, M. E., and Russell, J. M.: Two-dimensional model calculations of nitric oxide transport in the middle atmosphere and comparison with Halogen Occultation Experiment data, J. Geophys. Res., 102, 3527–3545, 1997.

Solomon, S. C.: Auroral particle transport using Monte Carlo and hybrid methods, J. Geophys. Res., 106, 107–116, 2001.

Torr, M. A., Torr, D. G., and Ong, R. A.: Ionization frequencies for major thermospheric constituents as a function of solar cycle 21, Geophys. Res. Lett., 6, 771–774, 1979.

Turunen, E.: EISCAT incoherent scatter radar observations and model studies of day to twilight variations in the D-region during the PCA event of August 1989, J. Atmos. Terr. Phys., 55, 767, 1993.

Turunen, E., Matveinen, H., Tolvanen, J., and Ranta, H.: D-region ion chemistry model, STEP Handbook of Ionospheric Models, (Ed) Schunk, R. W., SCOSTEP Secretariat, Boulder, Colorado, USA, 1–25, 1996.

Ulich, T., Turunen, E., and Nygrén, T.: Effective recombination coefficient in the lower ionosphere during bursts of auroral electrons, Adv. Space Res., 25, 47–50, 2000.

Verronen, P. T., Turunen, E., Ulich, T., and Kyrölä, E.: New possibilities for studying ozone destruction by odd nitrogen in the middle atmosphere through GOMOS and MIPAS measurements, in Proc. European Symposium on Atmospheric Measurements from Space (ESAMS'99), vol. 2, European Space Agency, ESTEC, Noordwijk, The Netherlands, 607–610, 1999.

WMO: Global ozone research and monitoring project - Report no. 16: Atmospheric Ozone 1985, World Meteorological Organization, Geneva, Switzerland, 1985.

Zadorozhny, A. M., Tuchkov, G. A., Kikthenko, V. N., Laštovička, J., Boška, J., and Novák, A.: Nitric oxide and lower ionosphere quantities during solar particle events of October 1989 after rocket and ground-based measurements, J. Atmos. Terr. Phys., 54, 183–192, 1992.